

Generation and Initial Characterization of FDD Knock In Mice

Luca Giliberto^{1‡}, Shuji Matsuda¹, Ruben Vidal², Luciano D'Adamio^{1*}

1 Department of Microbiology and Immunology, Albert Einstein College of Medicine, Bronx, New York, United States of America, **2** Department of Pathology and Laboratory Medicine, Indiana Alzheimer Disease Center, Indiana University School of Medicine, Indianapolis, Indiana, United States of America

Abstract

Background: Mutations in the integral membrane protein 2B [1], also known as *BRI*₂ [2], a type II trans-membrane domain protein cause two autosomal dominant neurodegenerative diseases, Familial British and Danish Dementia [3]. In these conditions, accumulation of a C-terminal peptide (ABri and ADan) cleaved off from the mutated precursor protein by the pro-protein convertase furin [4], leads to amyloid deposition in the walls of blood vessels and parenchyma of the brain. Recent advances in the understanding of the generation of amyloid in Alzheimer's disease has led to the finding that *BRI*₂ interacts with the Amyloid Precursor Protein (APP), decreasing the efficiency of APP processing to generate Aβ [5,6,7]. The interaction between the two precursors, APP and *BRI*₂, and possibly between Aβ and ABri or ADan, could be important in influencing the rate of amyloid production or the tendency of these peptides to aggregate.

Methodology/Principal Findings: We have generated the first *BRI*₂ Danish Knock-In (FDD_{KI}) murine model of FDD, expressing the pathogenic decamer duplication in exon 6 of the *BRI*₂ gene. FDD_{KI} mice do not show any evident abnormal phenotype, with normal brain histology and no detectable amyloid deposition in blood vessel walls or parenchyma.

Conclusions/Significance: This new murine mouse model will be important to further understand the interaction between APP and *BRI*₂, and to provide insights into the molecular basis of FDD.

Citation: Giliberto L, Matsuda S, Vidal R, D'Adamio L (2009) Generation and Initial Characterization of FDD Knock In Mice. PLoS ONE 4(11): e7900. doi:10.1371/journal.pone.0007900

Editor: Richard Mayeux, Columbia University, United States of America

Received: July 22, 2009; **Accepted:** October 26, 2009; **Published:** November 18, 2009

Copyright: © 2009 Giliberto et al. This is an open-access article distributed under the terms of the Creative Commons Attribution License, which permits unrestricted use, distribution, and reproduction in any medium, provided the original author and source are credited.

Funding: The funders had no role in study design, data collection and analysis, decision to publish, or preparation of the manuscript. This work was supported in part by Alzheimer Disease Research Grant A2003-076 (LD); National Institutes of Health Grants RO1 AG22024 (LD); RO1 AG21588 (LD); R21 AG027139 (LD); American Health Assistance Foundation A2008-304 (RV).

Competing Interests: LG and LD are inventors of an AECOM patent on the FDD mice. The mice discussed in this paper (*BRI*₂-ADan knock-in mice) are patent-pending. The assign is the Albert Einstein College of Medicine. The Albert Einstein College of Medicine has licensed the patent to a Biotech company (Remegenix) of which Dr. D'Adamio is a co-founder. This does not alter the authors adherence to all the PLoS ONE policies on sharing data and materials, as detailed online in the guide for authors <http://www.plosone.org/static/policies.action#sharing>.

* E-mail: luciano.dadamio@einstein.yu.edu

‡ Current address: The Litwin-Zucker Research Center for the Study of Alzheimer's Disease, The Feinstein Institute for Medical Research, North Shore – LIJ, Manhasset, New York, United States of America

Introduction

*BRI*₂ is a type II trans-membrane protein of unknown function. The *BRI* gene belongs to a multigene family comprising at least three homologues in both mice and humans, *BRI*₁, *BRI*₂ and *BRI*₃ (also referred to as *ITM2A*, *ITM2B* and *ITM2C*, or *E25A*, *E25B* and *E25C*, respectively) [1,2,3,8,9]. It possesses a BRICHOS domain, a conserved motif common to members of the *BRI*, *ChM-I*, *SP-C* and *CA11* protein families, thought to have a role in the targeting of the respective proteins to the secretory pathway or to intracellular processing [10]. Proteins sharing the BRICHOS motif are dissimilar, and associate with a diverse range of phenotypes, varying from dementia to cancer and respiratory distress.

*BRI*₂ was first described in relation to Familial British Dementia (FBD) [2], an autosomal dominant neurodegenerative disease characterized by the early onset of personality changes, memory and cognitive deficits, spastic rigidity and ataxia. In FBD, a C-terminal 34 amino acid (aa) peptide of *BRI*₂ accumulates as amyloid, leading to severe amyloid angiopathy of the brain and

spinal cord with perivascular amyloid plaque formation, parenchymal plaques affecting the limbic areas, cerebellum, cerebral cortex, neurofibrillary tangles of hippocampal neurons and periventricular white matter changes [11]. Familial Danish Dementia (FDD), previously known as hereditary ophthalmotoencephalica, is an autosomal dominant disease characterized by the accumulation of an amyloidogenic C-terminal 34 aa peptide of *BRI*₂ [3]. FDD is characterized by early onset cataracts, deafness, progressive ataxia and dementia [3,12]. Neuropathological examination of patients with FDD shows diffuse brain atrophy with a particularly severe involvement of the cerebellum, cerebral cortex and white matter, as well as the presence of very thin and almost demyelinated cranial nerves, and widespread amyloid angiopathy in the small blood vessels and capillaries of the cerebrum, choroid plexus, cerebellum, spinal cord and retina. In FDD, parenchymal compact plaques are consistently absent, whereas neurofibrillary tangles (NFTs) are the major histological finding in the hippocampus [3,12].

*BRI*₂ is physiologically cleaved, at the C-terminus, by furin, a calcium-dependent serine endoprotease, producing a 23 aa soluble

C-terminal fragment. FBD and FDD are due to mutations in the *BRI₂* gene located on chromosome 13q14 [2,8]. In FBD, a single base substitution at the stop codon of *BRI₂* generates a longer open reading frame, resulting in a larger, 277 aa precursor (*BRI_{2-ABri}*, compared to the 266 aa long normal protein) [2]. In FDD, a decamer duplication in the 3' region of the *BRI₂* gene, right before the stop codon, leads as well to the production of a longer, 277 aa protein (*BRI_{2-ADan}*) [3]. The genetic defect is different, but the outcome is the same: the generation of a longer 34 aa C-terminal fragment, ABri in FBD and ADan in FDD, which accumulates as amyloid [2].

Several neuropathological features are common to FBD, FDD and Alzheimer's disease (AD): amyloid deposition and neurodegeneration in the central nervous system (CNS), accumulation of complement proteins and their pro-inflammatory activation products, including iC3b, C4d, Bb, and C5b-9, neurofibrillary pathology and hyperphosphorylated tau [12,13,14]. Furthermore, in FDD, Alzheimer's A β co-deposits with ADan, mainly in vascular and perivascular amyloid lesions and less in parenchymal preamyloid deposits [12], while compact plaques are not frequent [2,12,15].

More recently, a new link between *BRI₂* and A β has been found. It has been shown that *BRI₂* binds APP in a region comprising the extracellular juxtamembrane domains of both proteins, in a cis fashion [5,6,7]. This interaction leads to interference on the physiological processing of APP: *BRI₂* restricts the docking of γ -secretase to APP and the access of α - and β -secretases to their cleavage site on APP itself. The overall result of this interaction is the reduction of the amyloidogenic processing of APP, without a direct inhibition of the general activity of the secretases [5]. *BRI₂* maturation is required for this function. In fact, only m*BRI₂* (and not the immature precursor) binds mature APP and inhibits its processing on the plasma membrane and in endocytic compartments [16]. Matsuda et al have further shown that *BRI₃*, a member of the *BRI* family, binds and inhibit the action of α - and β -secretases on APP [17]. Others have argued that the *BRI₂*-23 wild type C-terminal peptide, released from *BRI₂* by furin/furin-like cleavage, can inhibit A β aggregation in vitro [18].

The interaction between these two amyloidogenic proteins can be of interest, especially for the design of new therapeutic strategies for AD and FBD/FDD. To this end, the processing of the *BRI₂* precursor, both in the wild type allele and its mutant form must be understood. Transgenic mice bearing the British or Danish mutations have been generated, and are under investigation as models of dementias and cerebral amyloid angiopathies [19,20]. A transgenic FDD model which over-expresses the Danish mutant form of *BRI₂* shows amyloid deposition in the walls of blood vessels of the cerebrum and cerebellum, parenchymal amyloid deposition and reactive gliosis, ADan amyloidosis and some signs of cerebellar ataxia [20]. Transgenic over-expression of human mutant genes has been extensively used to generate mouse models for human neurodegenerative disorders due to the need of over-expressing enough amount of the mutant protein in order to observe a phenotype. It is however possible that some disorders may, at least partially, be due to loss of function rather than a gain of toxic function due to mutations. If this were the case, a transgenic approach would be counterproductive. Therefore, we have reasoned that models reproducing the genetics of human pathologies may be worth studying since they may unveil important disease mechanisms that a transgenic approach may miss or, possibly, hide. Thus, we have generated a genetically faithful model of FDD by introducing the pathogenic human mutation in the mouse *BRI₂* gene by a knock-in technology. Here,

we describe the generation of this Knock-In murine model of FDD (*FDD_{KI}*) and its initial characterization.

Materials and Methods

Ethics Statement

Mice were maintained on a C57BL/6 background for several generations (at least 15). Mice were handled according to the Ethical Guidelines for Treatment of Laboratory Animals of Albert Einstein College of Medicine. The procedures were described and approved in animal protocol number 20040707.

FDD_{KI} Mice Construction

To clone the ADan mutation allele, a fragment obtained from BAC (containing mouse *BRI₂* genome) was amplified by PCR with the following primers:

Fw: 5'-cccAAGCTTtttttttttttaagacaac-3'; Rev: 5'-gggAAGCTTgaagtgtcagcaggag-3', obtaining a 7536 bp fragment, flanked by 2 *HindIII* sites, and comprising part of Intron 2 to a 3'UTR region, up to 3850 bp from the *BRI₂* stop codon. Such a fragment was cloned into a pBS vector, into *HindIII* sites (pBS-Ex3-6 *HindIII*), and used as a *template* for subsequent cloning.

A 340 bp fragment containing the ADan (duplication 786–795 of cDNA) mutation, plus a humanizing substitution a \rightarrow g (acc \rightarrow gcc = Threonine \rightarrow Alanine) at the 12th codon of exon 6, was obtained by serial PCRs, using pBS-Ex3-6 *HindIII* as a template. The final external primers contained restriction sites for *HincII* (5') and *EcoRI* (3'). The mutated fragment (*HincII*-ADan-*EcoRI*) was inserted into the *SmaI* and *EcoRI* sites of a pBS vector yielding pBS-ADan0.3.

Subsequently, 2 *EcoRI*-*EcoRI* and *EcoRI*-*XhoI* fragments (2.6 kbp total) were cut from the template and added 3', in tandem, to pBS-ADan0.3, generating pBS-ADan2.9, containing the Right Arm (RA) fragment of the construct.

A *NotI*-*XhoI* fragment from pBS-ADan2.9, comprising the RA, was inserted into *NotI* and *SacII* sites of a Soriano PGK-Neo-dTA vector (blunt-ended by the *SacII* and *XhoI* digestion followed by treatment of T4-exonuclease and Klenow polymerase respectively) at 5' of the Neo cassette. The *XhoI* site was reconstituted upon ligation of the fragment into the vector.

The construct's Left Arm was extracted from the template with *EcoRI* and *HincII*, generating a 1.1 kbp into Intron 5 up to the corresponding *HincII* site, 5' of Exon 6 (start of Right Arm). The fragment was thus inserted into the PGK-Neo-dTA vector at 3' of the Neo cassette and 5' of the dTA cassette.

The resulting construct was thus:

---Right Arm-LoxP1-PGK-Neomycin cassette-LoxP2-Left Arm-dTA cassette---

The resulting construct was linearized with *SalI* and purified prior to injection in ES cells strain 129 by electroporation. ES culture was performed on feeder layer, and further electroporation and handling was also performed according to the methodology employed at Dept of Cell Biology, Albert Einstein College of Medicine, and according to Wakayama et al. [21]. In particular, after electroporation, ES cells were re-plated in 55 cm² dishes and let grow until visible clones would appear. Clones were then picked and transferred to 96 well plates in triplicates. Triplicates were either screened by PCR or frozen for subsequent use and further analysis.

Homologous recombinants were selected with G418 (200 μ g/ml) and dTA exclusion.

Injection of the two Danish ES cell clones into C57BL/6J blastocysts was performed at the Albert Einstein College of Medicine gene-targeting facility, according to the current facility

protocol (<http://www.aecom.yu.edu/home/SharedFacilities/ViewFacility.asp?ID=30>).

PCR Analysis

The PCR screening was performed using the Expand Long Template PCR System (Roche-applied-Science) with Betaine, according to the manufacturer instructions. PCR analysis of recombinant ES cells and mice was conducted with the following primers and digestion strategies to identify the correct recombinant clones and strains:

ES cells:

Left arm:

Genomic primer: 5'-CAGTCCTACCTTATCCATGAGCAC-3'

Neo cassette primer: 5'-CTTCCTCGTGCTTTACGGTATC-3'

Product: 1637 bp

Right arm:

Genomic primer: 5'-AGTCTGTATCTCACTACGGCATC-C-3'

Neo cassette primer: 5'-TGCACGAGACTAGTGAGACGT-G-3'

Product: 3403 bp

Amplification of the inserted construct and digestion:

Genomic upstream primer: 5'-CAGTCCTACCTTATCCATGAGCAC-3'

Genomic downstream primer: 5'-AGTCTGTATCTCACTACGGCATCC-3'

Product: 4300 bp = construct without Neo cassette; NotI digestion → 2900 bp + 1300 bp

Product: 6109 bp = construct with Neo cassette; NotI digestion → 3100 bp + 2900 bp

Mice:

Whole construct

Set 1

Fw primer: 5'-ATGGCACCACCCACAATAGG-3'

Rev primer: 5'-CCTAGCAACTGGTAACAGTGC-3'

Product: 2027 bp with Neo cassette

Product: 332 bp without Neo cassette

Product: 194 bp wild type

Set 2

Fw primer: 5'-ATGGCACCACCCACAATAGG-3'

Rev primer: 5'-ggtaagctctaaggagaagcg-3'

Product: 2500 bp with Neo cassette

Product: 849 bp without Neo cassette

Product: 704 bp wild type

Due to the specific sequences present in the amplified PCR product, no digestion of the amplicon could be performed on the mice PCR analysis. PCR products were thus sequenced to ascertain that the targeted sequence was correctly inserted in the genomic DNA. The sequence has been deposited in GenBank (accession number GQ424832).

Southern Blot Analysis

Twenty µg of genomic DNA was digested with *Bam*HI overnight, run on a 1% TAE agarose gel and transferred on a Hybond-N+ membrane (Amersham).

The probe was prepared by PCR from a BAC clone (RP24) with the following primers:

-Left arm:

Fw: 5'-GACAGAGGTTCTGCCCTCAG-3'

Rev: 5'-ACCGAGTCGTAGGACAGTG-3'

Probe size: 547 bp

-Right arm:

Fw: 5'-CTGTGCTGCCTGACACTACTTC-3'

Rev: 5'-TCTGTCCATACTCCCTGTCCCTT-3'

Probe size: 515 bp.

One µg of PCR probe was labelled with 5 µL of ³²P-dCTP (3000 Ci/mmol, ICN) and purified through a Push Column (Stratagene) according to the manufacturer's protocol. Membranes, containing the cleaved genomic DNA, were hybridized at 65°C and subsequently washed 4 times in SSC buffer (Sigma). Film was exposed to the hybridised membranes at -80°C and then developed.

General Pathology Analysis

Wild-type and FDD_{KI} animals were studied at 18 months of age. After anesthesia, animals were perfusion-fixed with 4% paraformaldehyde in 0.1 M phosphate buffer (pH 7.2) (Sigma), after which brains and organs were removed, embedded in paraffin and sectioned. Eight µm sections were cut and mounted on poly-l-lysine-coated slides. After deparaffinization in Xylene and rehydration, sections were stained with hematoxylin and eosin (H&E), Congo red standard methods. Mineralization was visualized in H&E sections as a deep basophilic amorphous and/or granular material.

Brain Histology and Immunohistochemistry

Wild-type, FDD_{KI} and FDD-Tg animals were studied at 18 months of age. After anesthesia, animals were perfusion-fixed with 4% paraformaldehyde in 0.1 M phosphate buffer (pH 7.2) (Sigma), after which brains were removed, embedded in paraffin and sectioned. Eight µm sections were cut and mounted on poly-l-lysine-coated slides. Sections were stained with H&E, Congo red and Thioflavin S (ThS) methods. Immunohistochemical stainings were carried out as described [20] with following primary antibodies: glial fibrillary acidic protein (GFAP) (Dako, Carpinteria, CA); ubiquitin (Dako); amyloid β protein (Aβ) clone 4G8 (SIGNET, Dedham, MA); and ADan amyloid peptide (Ab 1700) [20]. Immunostaining was visualized using the avidin-biotin system (Vectastain; Vector Laboratories, Burlingame, CA) and 3,3'-diaminobenzidine (Sigma) as the chromogen. The sections were counterstained with cresyl violet or H&E. ADan transgenic (FDD-Tg) mice were described elsewhere [20].

Neuronal Cultures

Neuronal cultures of FDD_{KI} mice, and wt littermates, were performed as described previously [22,23] from E16-17 fetuses.

Western Blot

Western blot was conducted on protein extracts from brains or neuronal culture of FDD_{KI} mice and wt littermates, as described previously [5] for cells lysates and brain tissue. Briefly, primary neuronal cells were lysed in Hepes-Triton buffer (20 mM Hepes/NaOH pH 7.4, 1 mM EDTA, 150 mM NaCl, 0.5% Triton X-100, plus protease inhibitors (PIs)) on ice for 30 min. The lysates were cleared by spinning at 20,000 g for 10 min. Equal amount of proteins of cleared lysates were loaded on SDS-PAGE and transferred onto nitrocellulose membranes; APP and BRI₂ (wild type and Danish mutants) were detected by 22C11 (Chemicon, MAB348) or BRI₂ antibody, generously provided by Dr. Haruhiko Akiyama, respectively [24].

Results

Generation and Characterization of FDD_{KI} Mice

The targeting strategy for the generation of the Danish mutant FDD_{KI} mice entailed the replacement of the BRI₂ exon 6 with a mutated exon 6 carrying the FDD mutation. We generated a

targeting vector for the introduction of FDD BRI_2 mutation. The vector used the floxed $PGK-neo$ selection cassette and contains a 5' homologous region and the negative selection cassette, $PGK-dt$. The 3' homologous region introduced the FDD mutation and a $BamHI$ site into the BRI_2 mouse gene. The 10 nucleotide insertion found in patients with FDD was introduced before the stop codon. In order to humanize the mouse C-terminal region of BRI_2 , an alanine (A) was substituted for threonine (T) at codon 250 (Fig. 1a) of the murine BRI_2 gene.

The linearized targeting vector was transfected into 129 ES cells by electroporation. In the presence of the positive selection drug, G418, only those clones in which the $PGK-neo$ selection cassette was integrated and the $PGK-dt$ cassette was removed by homologous recombination would survive. ES cell clones carrying the targeting vector by random, non-homologous integration, were eliminated due to expression of diphtheria toxin.

After selection in G418-containing medium, ES cell clones carrying the proper homologous recombination and the $tADan$ (targeted ADan) allele were identified by PCR for 5' region (i.e. Left Arm: if homologous recombination had occurred these primers would amplify a product of 1.67 kb) and for the 3' region (i.e. Right Arm: if homologous recombination had occurred these primers would amplify a product of 3.4 kb). Out of the ~600 screened ES clones, we found three clones in which the Danish mutation was

inserted in one of the BRI_2 alleles. Representative positive ($BRI_2^{tADan/+344}$ and $BRI_2^{tADan/+339}$) and negative ($BRI_2^{tADan/+342}$) ES clones are shown in Fig. 1b. Also, PCR amplification and digestion, as specified in the Material and Methods section, was used to check the proper insertion of the construct in the genomic DNA and the removal of the Neo cassette (not shown).

The occurrence of homologous recombination was confirmed by sequencing the PCR products and by performing Southern blot analysis (Fig. 1c). DNA derived from individual $BRI_2^{tADan/+}$ ES clones was digested with $BamHI$, gel separated, blotted into a nylon membrane and hybridized with either the 5' or the 3' probe. The 5' probe hybridizes with a ~11.9 kb fragment derived from the wild-type locus. Homologous recombination at the 5' homologous region yields a ~8.9 kb fragment upon $BamHI$ digestion due to the introduction of the $BamHI$ site and the $PGK-neo$ selection cassette. ES clones $BRI_2^{ADan/+344}$ and $BRI_2^{ADan/+339}$ carry a wild type allele (11.9 kb) and a recombined allele (8.9 kb). Of note, the 11.9 kb and 8.9 kb bands had a similar intensity, indicating that 50% of the BRI_2 alleles are wild type and 50% are recombined, and proving that the ES cells we have selected are a clonal populations. Similar results were obtained when homologous recombination at the 3' site was assessed. In this case the 3' probe detected a wild-type ~11.9 kb fragment and a recombinant 4.7 kb fragment, due to the introduction of the $BamHI$ site.

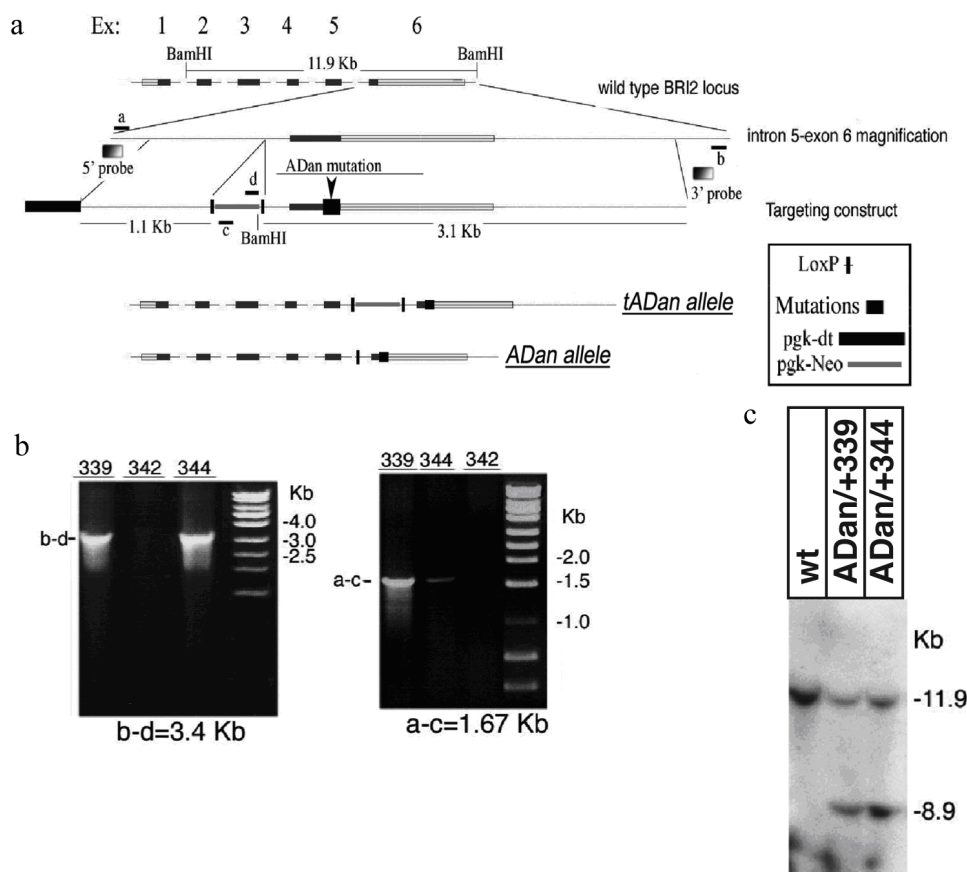


Figure 1. Generation of FDD_{KI} mice. 1a. Schematic representation of the construct that was injected in 129 ES cells, showing site of ADan mutation on Exon 6, primer sites, site of Southern Blot probe, LoxP, pgk-dt and pgk-Neo sites. The bottom graphics depict the construct with and without the pgk-Neo cassette that has been removed by means of Cre recombinase. 1b. Examples of 2 ES clones positive for the homologous recombination of the mutated allele: left arm (a-c: 1.67 kb) and right arm (b-d: 3.4 kb) PCRs are shown. 1c. Southern Blot showing a shift from the 11.9 kb of the wild type genome to the 8.9 kb band of the FDD KI mice, due to the insertion of a new $BamHI$ site. KI mice show both bands, indicating heterozygosity.

doi:10.1371/journal.pone.0007900.g001

These two Danish ES cell clones (129, agouti coat colour), carrying the correct site-specific homologous recombination, were injected into C57BL/6J blastocysts (black coat colour) at the Albert Einstein College of Medicine gene-targeting facility. The resulting chimeras with a high proportion of agouti coat colour (*i.e.* with a high relative contribution from the injected ES cells) were backcrossed to C57BL/6J mice to obtain heterozygous $BRI_2^{ADan/wt}$, which were identified by PCR and Southern analysis as described above (not shown) using tail DNA. Heterozygous mice were crossed to Meu40-Cre mice to obtain Meu40/ $BRI_2^{ADan/wt}$ animals. Cre is a bacteriophage P1-encoded recombinase that catalyzes site-specific recombination between two 34 bp loxP recognition sites, resulting in the excision of the intervening DNA sequences. The resulting mouse has been named FDD_{KI}.

General Characteristics and Pathology of the FDD_{KI} Mice

Mice presented with no growth abnormalities, thrived at appropriate age, as their wild type littermates. Up to age 18 months, no susceptibility to infections was noted. The animals are active and alert.

Before the pathology examination, at 18 months of age, they presented in good body condition with adequate body fat, with no discharges or secretions from nostrils, conjunctiva, aural, urogenital or anal openings. Some mice also presented heart valve melanosis, which is a common finding in aged mice of various strains. Other sporadic findings, which are common in aged mice, were small foci of hepatocellular necrosis, vacuolation of and degeneration/regeneration of kidney tubular epithelial cells, mineralization in the kidney tubules in the pelvis and cortico-medullary junction (not

shown). Overall, these mice have lesions that are commonly found in older mice and are considered age-related, spontaneous lesions. All of the lesions found were considered to be within the normal limits for age-related lesions. One of the animals presented with a uterine histiocytic sarcoma and hydronephrosis, both of which are found in older, untreated mice at low incidence.

Neuropathology

A few animals presented a small amount of dark basophilic material deposited on either side of the lateral thalamus consistent with mineralization (incidental, Fig. 2d), which is a common finding in aged mice of various strains, and the deposits develop along the basement membranes of the vasculature and may contain calcium and phosphorus. The finding of dark brown pigment along the meninges of the olfactory bulbs is consistent with melanosis (incidental, Fig. 2a), which is also a common finding in mice in dark pigment mouse strains such as C57BL/6 or having that strain the their background. All the brain tissue and the spinal cord were stained with Congo red for potential amyloid deposition. All of the stained tissue was negative for amyloid (not shown). Samples of H&E staining of cerebral cortex, hippocampus, cerebellum, thalamus and spinal cord are shown in Fig. 2a–e.

Brain sections of 18-month-old mice were examined for FDD-related pathology, particularly for amyloid deposition in brain parenchyma and vessel walls. For comparison, we included sections of an age-matched female FDD-Tg mouse, which expresses the Danish mutant form of human BRI_2 under the mouse prion protein promoter [20]. H&E staining of Knock In mice (Fig. 3c, 4a) showed no significant loss of neurons or

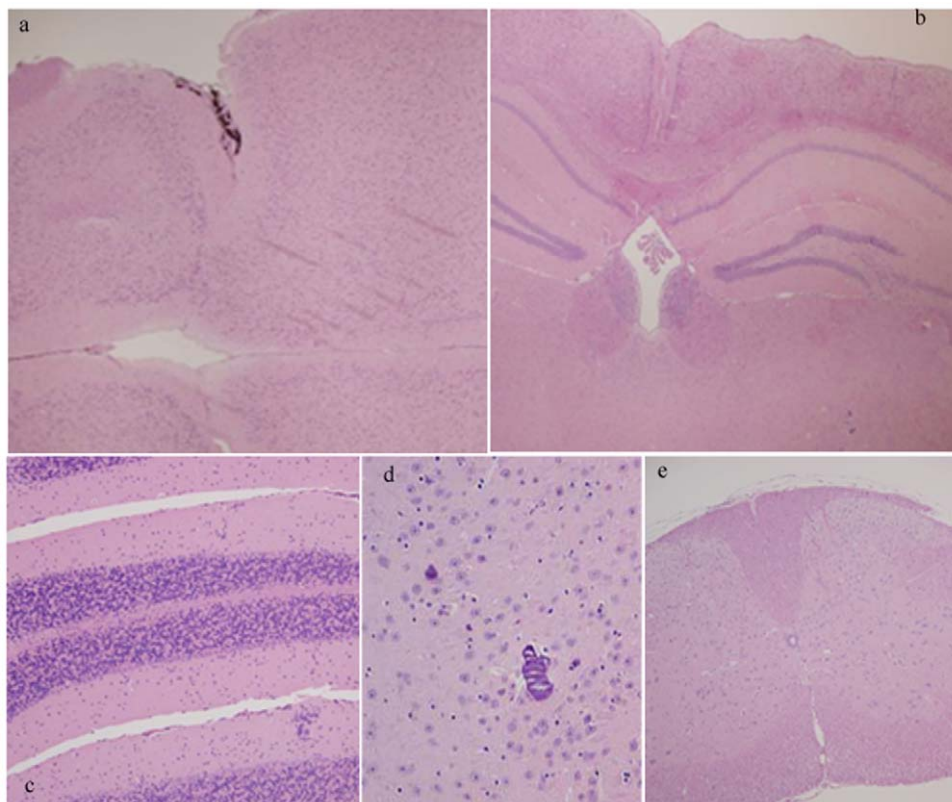


Figure 2. General Neuropathology. H&E staining of 18 month old FDD_{KI} mice showing signs of melanosis in the meninges of olfactory bulb (a) and signs of mineralization in the thalamus (d). The remaining parenchyma of brain cortex and hippocampus (b), cerebellum (c) and spinal cord (e) show normal cellular structures.

doi:10.1371/journal.pone.0007900.g002

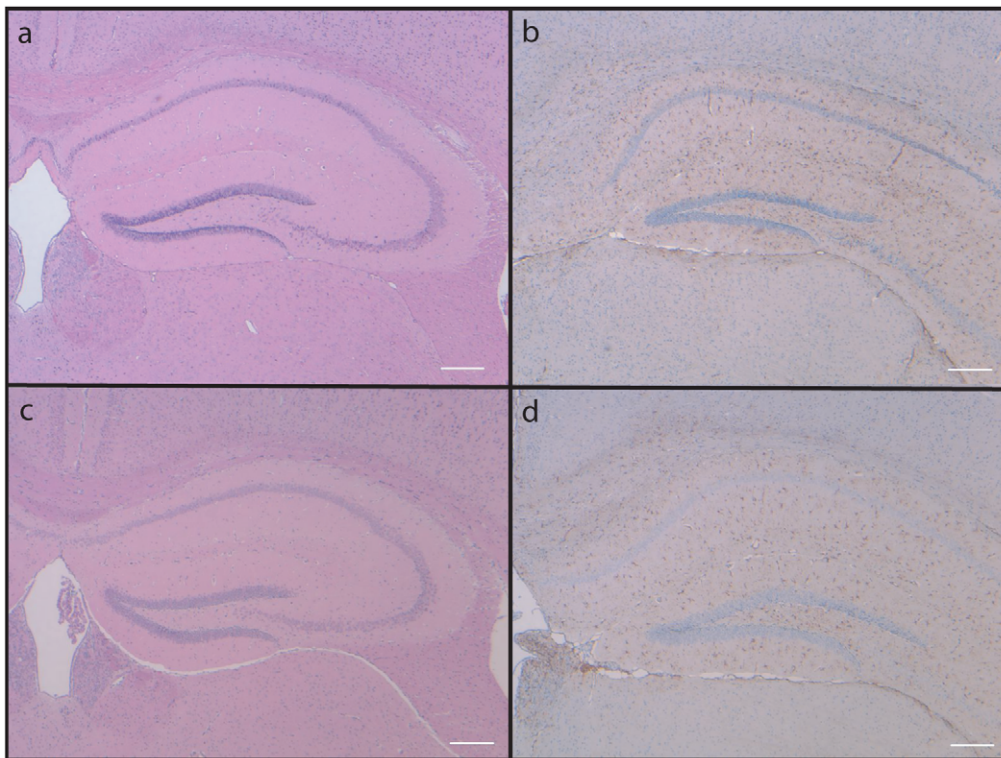


Figure 3. Sections of the hippocampus of FDD_{KI} mice. Sections from a wild type (a, b) and a homozygous knock-in mouse (c, d) were stained with H&E (a, c). Sections were also studied by immunohistochemistry using anti-GFAP (b, d). No significant differences were observed between wild-type and Knock In mice. Scale bars: a–d, 200 μ m. doi:10.1371/journal.pone.0007900.g003

noticeable malformations, and this observation was further confirmed when mutant sections were compared with those of wild type littermates (Fig. 3a, 4d). Immunostaining using anti-GFAP (Fig. 3b, d) and anti-ubiquitin (not shown) antibodies did not reveal significant differences with wild type mice in levels of activated astrocytes or presence of ubiquitinated material, respectively. Staining using Congo red or ThS did not show the presence of amyloid deposits (Fig. 4b). Amyloid deposition in FDD-Tg mice is particularly strong in the cerebellum (Fig. 4e) but not in Knock In mice (Fig. 4b) and only FDD-Tg mice showed immunoreactivity using Ab 1700, specific for the ADan amyloid peptide [20] (Fig. 4f versus 4c). Immunoreactivity was not seen in non-transgenic littermates, FDD-Tg and Knock In mice using antibody 4G8 (not shown). These results indicated that the brain of Knock In mice maintained normal morphology of aged mice and were free of amyloid deposits at 18 months of age.

Biochemical Analysis of BRI_{2-ADan} Expression

To determine whether the mutant proteins are expressed *in vivo*, we made protein extracts from neuronal cultures of wt, $BRI_2^{ADan/wt}$ and $BRI_2^{ADan/ADan}$ mice. Western blot analysis of these samples shows three phenomena. 1) A common, major band of about 32 kDa is readily visible in all three samples. This band corresponds to the post-furin cleavage mature BRI₂ (mBRI₂) polypeptide because mBRI₂ is identical regardless of whether it is derived from the wild type or the mutant precursor protein. 2) A much less abundant protein of \sim 33 kDa which is visible in the wild type and $BRI_2^{ADan/wt}$ sample but not the $BRI_2^{ADan/ADan}$ lysate. This band corresponds to the wild type, immature BRI₂ precursor (imBRI₂). The absence of this band in the $BRI_2^{ADan/ADan}$ neurons is attributable to the fact that these cells have both BRI₂ alleles

mutated. 3) As expected, the $BRI_2^{ADan/wt}$ sample expresses all three BRI₂ polypeptides, i.e. wild type imBRI₂, BRI_{2-ADan} precursor and mBRI₂. It is worth noting that, while immature murine BRI₂ (imBRI₂) is barely detectable, BRI_{2-ADan} is more markedly expressed (see $BRI_2^{ADan/ADan}$ neurons, Figure 5) in this specific experiment. Whether this is related to the artificial absence of the wild type protein (this does not happen in FDD since the patients have only one mutated allele) or reflects some interesting biology of BRI_{2-ADan}, remains to be determined. Notably, APP expression and maturation are comparable in FDD_{KI} and wt mice (Fig. 5, lower panel).

Discussion

In this manuscript we present an initial characterization of a Knock In model for a human neurodegenerative disorder, FDD. This Knock In model is strategically different from the conventional genetic approach to cerebral amyloidosis. Traditionally, mouse models for human dementias are based on a transgenic approach in which human mutant proteins that cause familial forms of dementia are over-expressed under the control of brain-specific promoters [25,26,27]. This approach has both limitations and advantages. The potential limitations are linked to the fact that these models are genetically incongruous with the human diseases. These dementias have an autosomal dominant way of transmission and affected subjects have a wild type and a mutant allele. On the contrary, the commonly used animal models over-express, from an artificial promoter, several copies of a mini-gene coding the mutant protein. The mutant gene is therefore expressed in a spatio-temporal manner different from the natural alleles and in cells with two copies of wild type alleles. However, transgenic

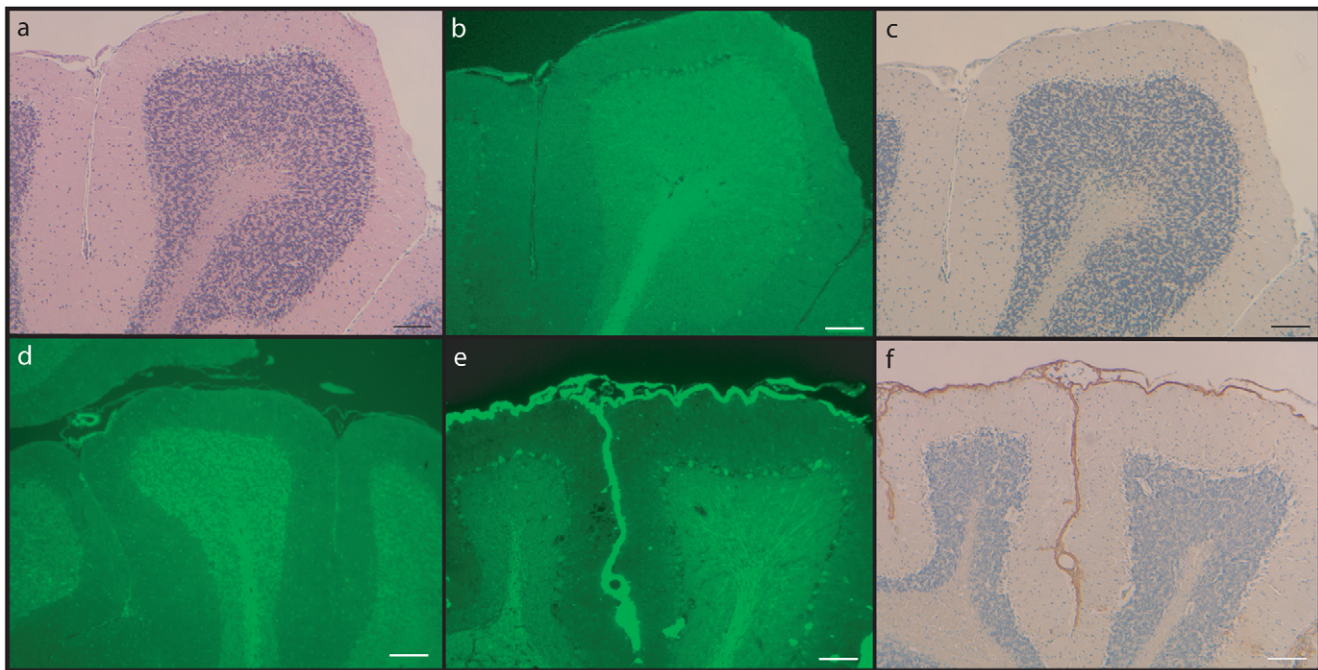


Figure 4. Sections of the cerebellum of FDD_{KI} mice. Sections from a wild-type (d), homozygous knock-in mouse (a–c), and FDD-Tg mouse (e, f) were stained with H&E (a) and ThS (b, d, e). Sections were also studied by immunohistochemistry using Ab 1700, specific for the ADan amyloid peptide (c, f). No significant differences were observed between wild-type and knock-in mice. Staining with ThS and Ab 1700 shows the presence of ADan amyloid only in FDD-Tg mice (e–f). Scale bars: a–e, 100 μ m; f, 200 μ m.
doi:10.1371/journal.pone.0007900.g004

approaches have successfully reproduced cerebral amyloidosis in mice, and the reproduction of those lesions is one of the main parameters used to endorse an animal model as representative of the human disease. The opposite is true for a Knock In approach. In this genetic paradigm, the pathogenic human mutation is inserted in the mouse allele. Thus, the Knock In mouse is genetically faithful to the human pathology. However, the Knock In model may not successfully reproduce the amyloid lesion in the mouse. The model that we present here is a clear demonstration of the above-mentioned assumptions. A comparison of the FDD-KI model that we have created with the FDD transgenic model generated by Vidal et al [20] illustrates the superior power of a

transgenic approach as far as the reproduction of amyloidogenic lesions are concerned.

In spite of this limitation, we believe that there is some merit to a Knock In approach. Human familial dementias may have a pathogenic component due to loss of function caused by the mutation [28,29,30,31,32]. This component may participate to the pathogenic process together with a gain of toxic function due to amyloidosis. A loss of function phenotype would be hidden by a transgenic approach for two reasons: 1) the two endogenous wild type alleles can support synthesis of sufficient amounts of functional wild type protein; 2) the over-expression of a partial loss of function mutant protein may augment rather than decrease that function, as may happen in the disease. It would be erroneous to assume that the absence of obvious neuropathological lesions (such as plaques, NFTs and/or neuronal cell loss) indicate absence of clinical pathology. Functional deficits may underlie the very first clinical manifestations of neurodegenerative diseases, and memory deficits may be caused not by gross anatomical changes but by subtle dysfunctions of the neuronal network. In this framework, determining the absence of neuropathological lesions in FDD_{KI} mice is intrinsically important. The behavioral characterization of this mouse model will test this hypothesis. In addition, the FDD_{KI} mouse will be useful to clarify the change of trafficking or processing of Danish mutant of BRI2 protein without potential artifacts due to over-expression in transgenic models. Finally, the FDD_{KI} mouse will be instrumental in studying the interaction between mutant BRI₂ and APP *in vivo* and how the Danish mutation affects the inhibitory role of BRI₂ on APP processing *in vivo*.

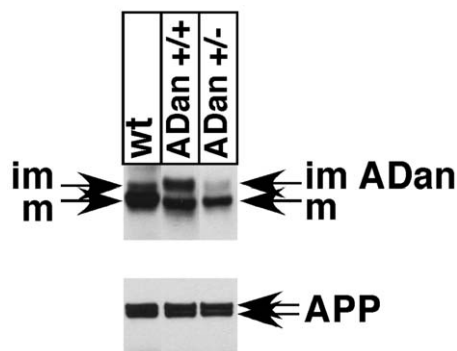


Figure 5. Biochemical analysis of BRI₂-ADan. Lysates from E16-17 neuronal cultures of wt, ADan +/- and ADan +/+ mice were blotted with antibodies against BRI2 and APP. Upper panel shows impaired maturation of BRI₂-ADan compared to wild type; lower panel show normal pattern of expression and maturation of APP.
doi:10.1371/journal.pone.0007900.g005

Acknowledgments

We thank Erhan Ma for the help in the genotyping and PCR procedures on the ADan KI mice; we thank Dr. Susan Newbigging MSc, DVM,

DVSc at the Toronto Centre for Phenogenomics, 25 Orde Street, Toronto ON M5T 3H7; we thank Dr. Bernardino Ghetti for the helpful discussion.

Author Contributions

Conceived and designed the experiments: LD. Performed the experiments: LG SM RV. Analyzed the data: LG RV LD. Wrote the paper: RV LD.

References

- Deleersnijder W, Hong G, Cortvrindt R, Poirier C, Tylzanowski P, et al. (1996) Isolation of markers for chondro-osteogenic differentiation using cDNA library subtraction. Molecular cloning and characterization of a gene belonging to a novel multigene family of integral membrane proteins. *J Biol Chem* 271: 19475–19482.
- Vidal R, Frangione B, Rostagno A, Mead S, Revesz T, et al. (1999) A stop-codon mutation in the BRI gene associated with familial British dementia. *Nature* 399: 776–781.
- Vidal R, Revesz T, Rostagno A, Kim E, Holton JL, et al. (2000) A decamer duplication in the 3' region of the BRI gene originates an amyloid peptide that is associated with dementia in a Danish kindred. *Proc Natl Acad Sci U S A* 97: 4920–4925.
- Kim SH, Wang R, Gordon DJ, Bass J, Steiner DF, et al. (1999) Furin mediates enhanced production of fibrillogenic ABri peptides in familial British dementia. *Nat Neurosci* 2: 984–988.
- Matsuda S, Giliberto L, Matsuda Y, McGowan EM, D'Adamo L (2008) BRI2 inhibits amyloid beta-peptide precursor protein processing by interfering with the docking of secretases to the substrate. *J Neurosci* 28: 8668–8676.
- Matsuda S, Giliberto L, Matsuda Y, Davies P, McGowan E, et al. (2005) The familial dementia BRI2 gene binds the Alzheimer gene amyloid-beta precursor protein and inhibits amyloid-beta production. *J Biol Chem* 280: 28912–28916.
- Fotinoupolou A, Tschaki M, Vlavaki M, Pouloupoulos A, Rostagno A, et al. (2005) BRI2 interacts with amyloid precursor protein (APP) and regulates amyloid beta (Aβ) production. *J Biol Chem* 280: 30768–30772.
- Pittois K, Wauters J, Bossuyt P, Deleersnijder W, Merregaert J (1999) Genomic organization and chromosomal localization of the Itm2a gene. *Mamm Genome* 10: 54–56.
- Vidal R, Calero M, Revesz T, Plant G, Ghiso J, et al. (2001) Sequence, genomic structure and tissue expression of Human BRI3, a member of the BRI gene family. *Gene* 266: 95–102.
- Sanchez-Pulido L, Devos D, Valencia A (2002) BRICHOS: a conserved domain in proteins associated with dementia, respiratory distress and cancer. *Trends Biochem Sci* 27: 329–332.
- Plant GT, Revesz T, Barnard RO, Harding AE, Gautier-Smith PC (1990) Familial cerebral amyloid angiopathy with nonneuritic amyloid plaque formation. *Brain* 113 (Pt 3): 721–747.
- Holton JL, Lashley T, Ghiso J, Braendgaard H, Vidal R, et al. (2002) Familial Danish dementia: a novel form of cerebral amyloidosis associated with deposition of both amyloid-Dan and amyloid-beta. *J Neuropathol Exp Neurol* 61: 254–267.
- Holton JL, Ghiso J, Lashley T, Rostagno A, Guerin CJ, et al. (2001) Regional distribution of amyloid-Bri deposition and its association with neurofibrillary degeneration in familial British dementia. *Am J Pathol* 158: 515–526.
- Rostagno A, Revesz T, Lashley T, Tomidokoro Y, Magnotti L, et al. (2002) Complement activation in chromosome 13 dementias. Similarities with Alzheimer's disease. *J Biol Chem* 277: 49782–49790.
- Tomidokoro Y, Lashley T, Rostagno A, Neubert TA, Bojsen-Moller M, et al. (2005) Familial Danish dementia: co-existence of Danish and Alzheimer amyloid subunits (ADan AND Aβ) in the absence of compact plaques. *J Biol Chem* 280: 36883–36894.
- Matsuda S, Matsuda Y, Snapp EL, D'Adamo L (2009) Maturation of BRI2 generates a specific inhibitor that reduces APP processing at the plasma membrane and in endocytic vesicles. *Neurobiol Aging*.
- Matsuda S, Matsuda Y, D'Adamo L (2009) BRI3 inhibits amyloid precursor protein processing in a mechanistically distinct manner from its homologue dementia gene BRI2. *J Biol Chem* 284: 15815–15825.
- Kim J, Miller VM, Levites Y, West KJ, Zwizinski CW, et al. (2008) BRI2 (ITM2b) inhibits Aβ deposition in vivo. *J Neurosci* 28: 6030–6036.
- Pickford F, Coomaraswamy J, Jucker M, McGowan E (2006) Modeling familial British dementia in transgenic mice. *Brain Pathol* 16: 80–85.
- Vidal R, Barbeito AG, Miravalle L, Ghetti B (2009) Cerebral amyloid angiopathy and parenchymal amyloid deposition in transgenic mice expressing the Danish mutant form of human BRI2. *Brain Pathol* 19: 58–68.
- Wakayama T, Rodriguez I, Perry AC, Yanagimachi R, Mombaerts P (1999) Mice cloned from embryonic stem cells. *Proc Natl Acad Sci U S A* 96: 14984–14989.
- Giliberto L, Zhou D, Weldon R, Tamagno E, De Luca P, et al. (2008) Evidence that the Amyloid beta Precursor Protein-intracellular domain lowers the stress threshold of neurons and has a “regulated” transcriptional role. *Mol Neurodegener* 3: 12.
- Giliberto L, Borghi R, Piccini A, Mangerini R, Sorbi S, et al. (2009) Mutant presenilin 1 increases the expression and activity of BACE1. *J Biol Chem* 284: 9027–9038.
- Akiyama H, Kondo H, Arai T, Ikeda K, Kato M, et al. (2004) Expression of BRI, the normal precursor of the amyloid protein of familial British dementia, in human brain. *Acta Neuropathol (Berl)* 107: 53–58.
- LaFerla FM, Oddo S (2005) Alzheimer's disease: Aβ, tau and synaptic dysfunction. *Trends Mol Med* 11: 170–176.
- McGowan E, Eriksen J, Hutton M (2006) A decade of modeling Alzheimer's disease in transgenic mice. *Trends Genet* 22: 281–289.
- Price DL, Wong PC, Markowska AL, Lee MK, Thinakaran G, et al. (2000) The value of transgenic models for the study of neurodegenerative diseases. *Ann N Y Acad Sci* 920: 179–191.
- Bentahir M, Nyabi O, Verhamme J, Tolia A, Horre K, et al. (2006) Presenilin clinical mutations can affect gamma-secretase activity by different mechanisms. *J Neurochem* 96: 732–742.
- De Strooper B (2007) Loss-of-function presenilin mutations in Alzheimer disease. Talking Point on the role of presenilin mutations in Alzheimer disease. *EMBO Rep* 8: 141–146.
- Wolfe MS (2007) When loss is gain: reduced presenilin proteolytic function leads to increased Aβ42/Aβ40. Talking Point on the role of presenilin mutations in Alzheimer disease. *EMBO Rep* 8: 136–140.
- Shen J, Kelleher RJ 3rd (2007) The presenilin hypothesis of Alzheimer's disease: evidence for a loss-of-function pathogenic mechanism. *Proc Natl Acad Sci U S A* 104: 403–409.
- Saura CA, Choi SY, Beglopoulos V, Malkani S, Zhang D, et al. (2004) Loss of presenilin function causes impairments of memory and synaptic plasticity followed by age-dependent neurodegeneration. *Neuron* 42: 23–36.